One-Step Processing of Highly Viscous Multiple Pickering Emulsions

*Faezeh Sabri, Wendell Raphael, Kevin Berthomier, Louis Fradette, Jason R. Tavares and Nick Virgilio**

Center for Applied Research on Polymers and Composites (CREPEC), Department of Chemical Engineering, Polytechnique Montréal, Montréal, Québec, H3C 3A7, Canada

* Corresponding author:

Phone: 1-514-340-4711 #4524

Fax: 1-514-340-4159

Email address: nick.virgilio@polymtl.ca

Postal address: Department of Chemical Engineering, Polytechnique Montréal, C.P. 6079 Succursale Centre-Ville, Montréal, Québec, H3C 3A7

KEYWORDS: Silica particles, Surface modification, Oil viscosity, Sodium alginate, Multiple Pickering emulsions

ABSTRACT

Hypothesis: solid-stabilized Pickering emulsions have attracted a lot of attention recently due to their surfactant-free character, and exceptional stability. At the moment, how the viscosities of the liquid phases impact the processing of Pickering emulsions remain to be clearly understood - it is however an important parameter to consider when developing chemical engineering processes employing these multiphase liquids. Our first assumption was that the amount of emulsified dispersed phase would drastically decrease as viscosity increases. *Experiments and Findings:* in this work, we demonstrate that double water-in-oil-in-water (W/O/W) Pickering emulsions are obtained in a single processing step when using very high viscosity silicone oils (≥ 10,000 cSt) and a single type of sub-µm silica particles modified with two grafted silanes and sodium alginate. The formation of water sub-inclusions proceeds via a phase-inversion mechanism. These sub-inclusions are subsequently stabilized and retained in the oil phase due to its viscosity, limiting sub-inclusions mobility, and the presence of adsorbed particles forming dense layers at oil-water interfaces, acting as barriers. The process we present is simple, requires a minimum number of components, and allows the preparation of multiple emulsions which could then be used to efficiently protect and/or transport a variety of sensitive encapsulated compounds.

Introduction

Multiple emulsions are multiphase fluids displaying a droplets-within-droplets type of dispersed phase. The simplest ones are "double emulsions", which are either water-in-oil-in-water (W/O/W) or oil-in-water-in-oil (O/W/O) systems [1, 2]. Multiple emulsions have a wide range of potential applications in fields such as the pharmaceuticals [3] and cosmetics [4, 5] industries, and food systems [6]. They can be used as carriers for the triggered release of encapsulated drugs, active compounds or sensitive molecules [7, 8], or as potential substitutes for red blood cells [9], to name a few.

Surfactants are typically employed to stabilize multiple emulsions: hydrophilic surfactants for the oil-in-water droplets, and hydrophobic surfactants for water-in-oil drops [10]. However, surfactants can desorb from interfaces if exposed to temperatures above 70°C, which can be undesirable, and can pose toxicity problems [11, 12]. Furthermore, when using surfactants, multiple emulsions are typically thermodynamically and kinetically unstable [13]. The kinetic barrier is caused by surfactant adsorption at the interface or the viscosity increase of the continuous phase between the droplets, while the thermodynamic barrier results from the considerable energy input required to disperse the surfactants [14]. Solid-stabilized emulsions, also known as 'Pickering' emulsions, can overcome these limitations [15]. Pickering emulsions involve solid particulates strongly adsorbing at fluid/fluid interfaces, stabilizing the droplets of a fluid dispersed in a second immiscible one, with the added benefit of avoiding the use of potentially harmful organic surfactants [16].

Multiple Pickering emulsions are most often produced via a two-step process and require two different and complementary interfacial stabilizers [17] – one hydrophilic, and one hydrophobic. During the first step of emulsification, a primary emulsion is produced with the first interfacial

stabilizer. Then, during the second emulsification step, this primary emulsion is in turn emulsified with the second stabilizer, resulting in a droplets-in-droplets dispersion. Microfluidic approaches [18, 19] using various flow-focusing [20, 21] techniques have also been developed to produce multiple emulsions via one step processes. However, these techniques typically display low production yields, limiting their industrial applications [22].

In order to obtain double Pickering emulsions, solid particles need to stabilize two different interfaces with different/complementary curvatures. Janus particles [10, 23-27], block copolymers [10, 13] and colloidal particles such as fumed silica particles [24, 25, 28] and bowl-like silicone resins [26] have been used to form multiple Pickering emulsions. Nanofibrillated cellulose and cellulose nanocrystals have also been used to produce Pickering double emulsions. Two types of nanocelluloses, pristine and surface-modified, have been used to form O/W/O emulsions [29]. In addition, the combination of surfactants with solid particles [30], amphiphilic copolymers [10] and various polymers such as poly(ethylene imine) [31], a commercial water-soluble polymer, grafted onto silica particles have been used to prepare multiple Pickering emulsions with low viscosity oils and solvents [22, 29, 32, 33]

Regarding the effect of viscosity (μ), previous studies [34-38] have demonstrated that the oil phase viscosity has an effect on the formation of Pickering emulsions, in particular on droplet size [36-39]. Increasing the viscosity of the dispersed oil phase typically results in the formation of larger droplets. However, the effect of viscosity remains only partially understood when it comes to the processing and formation of Pickering emulsions – especially for fluids with $\mu > 5{,}000$ cSt – and has not been investigated when it comes to the formation of multiple Pickering emulsions. The main objective of this work is to assess the impact of high viscosity oils on the processing and microstructure of solid-stabilized emulsions. Quite surprisingly, by using a single type of sub-μm

silica particles modified with surface-grafted sodium alginate (SA), a natural polysaccharide [40], we demonstrate that multiple emulsions are formed when the oil viscosity reaches a value of 10,000 cSt.

2. Experimental Section

2.1 Materials

Sub-µm silica particles (SP) with the following properties were kindly supplied by Nippon Shokubai Trading Co. : average diameter $d \approx 100$ nm, specific surface area $S = 72 \pm 3$ $m^2 \cdot g^{-1}$ (measured with a BET instrument model ASAP 2020 from Micromeritics Instrument Corporation). Trimethoxy(propyl)silane (TMPS, 97%), (3-aminopropyl)trimethoxysilane (APTMS, 97%), *N*-(3-dimethylaminopropyl)-*N'*-ethylcarbodiimide hydrochloride (EDC, > 98%), *N*-hydroxysuccinimide (NHS, 98%), alginic acid sodium salt (SA, from brown algae) (CAS. 9005-38-3, molecular weight ≈ 60 kDa, pKa = 3.5) [41], Na_2CO_3-$NaHCO_3$ buffer solution (pH 10.01), sodium azide (> 99%), and 5-(4,6-dichlorotriazinyl)aminofluorescein (DTAF) (D0531) were all purchased from Sigma-Aldrich and used without further purification. Ethanol (99.8%) was purchased from Thermo Fisher Scientific. Solutions of HCl 1 N and NaOH 12 N were of analytical grade and prepared without further purification with Milli-Q (DI) water (18.2 MΩ·cm, Synergy 185 system by Fischer Scientific). Silicone oils with a broad viscosity range (linear polydimethylsiloxane fluids, 10, 1,000, 5,000, 10,000 and 30,000 cSt) were purchased from Clearco Products Co., Inc.

2.2 Particle Surface Modification

2.2.1 Silanes Surface Grafting

In order to alter surface wettability and graft SA on silica particles, two different silanes were grafted simultaneously on the surface of silica particles. In a typical batch, as previously reported [42], 10 g of SP particles and 100 ml of a 95% v/v solution of ethanol and DI water were added in a hydrophobized erlenmeyer flask. The suspension was then stirred at 600-700 rpm with a magnetic stirrer, at room temperature [43]. The pH was maintained in-between 4.5 - 5.5 with HCl 1 N. 1.04 ml of APTMS (allowing the subsequent grafting of alginate) and 1.05 ml of TMPS (allowing control of particle surface wettability) were added simultaneously dropwise while stirring, following a targeted surface concentration of 10 molecules·nm^{-2} (5 molecules·nm^{-2} of APTMS, and 5 molecules·nm^{-2} of TMPS) [44]. The reaction was carried for 12 h and the particles were next collected by centrifugation (Sorvall RC 6+, Thermo Fisher Scientific) at 12,000 rpm for 20 min. The particles were cleaned by washing twice with ethanol to rinse off any remaining unreacted silane. The silane grafted particles, identified as SP-Sil, were dried at 70 ºC for 2 hrs in a vacuum oven.

2.2.2 Sodium Alginate Grafting

Part of the SP-Sil particles were next modified by grafting SA using a 1% w/v aqueous solution. 0.4 g of SA was first solubilized in 40 ml of DI water (1% w/v). 0.29 g of EDC and 0.17 g of NHS (EDC/NHS molar ratio = 1) were added to the SA aqueous solution (molar ratio of EDC/-COOH = 0.1, based on the quantity of SA's -COOH groups) [45]. 4 g of SP-Sil particles were next added to the solution and the pH was adjusted to 4.5 using HCl 1 N. The suspension was left to react at room temperature for 15 h, and the mixture was next centrifuged at 12,000 rpm for 20 min to collect the SA-modified particles, designated from this point as SP-SA particles. They were washed 3 times with DI water and dried at 70 °C for 10 h in a vacuum oven.

2.3 Particle Surface Characterization

2.3.1 Zeta Potential Measurements

The zeta potential (ζ) was measured with a Zetasizer Nano ZSP instrument (Malvern Instruments Ltd., Worcestershire, UK) for SP, SP-Sil and SP-SA particles. The particles were initially dispersed in DI water (pH adjusted in-between 2.0 to 10.0 with HCl 1 N or NaOH 12 N). The measurements were conducted at 25 °C at a particle concentration of 0.01 $g \cdot ml^{-1}$, on at least three different samples. All samples were freshly prepared before testing, and disposable folded capillary cells (DTS1070) were used. The electrophoretic mobility was determined and the Smoluchowski model was then applied using the instrument's software to obtain ζ [46].

2.3.2 Contact Angle and Oil Surface Tensions Measurements

The contact angles θ between water and particles, in air, were obtained with an OCA20 tensiometer (DataPhysics Instruments GmbH) at 25°C. The contact angles were directly measured on the surface of compressed pellets (0.1 g, 12 mm diameter and 0.5 mm thickness) made from SP or SP-SA particles, using a laboratory press (Model C 3100-212, Carver, laboratory Press, USA) applying a pressure of 70.2 MPa, which was maintained for 2 min once reached. Each pellet was then placed on the instrument and a ~4 µL droplet of DI water at the desired pH (2.0 to 10.0, adjusted using HCl 1 N or NaOH 12 N) was carefully placed on the surface of the compressed pellet using a syringe with an internal needle diameter of 0.52 mm (Hamilton, model 1750TLL, 500 µL). Images of the sessile water droplets on the pellets were automatically recorded every 0.1 s, until the drops completely penetrated into the pellets. The first images were used as values of the contact angles. For both SP and SP-SA particles, three compressed pellets were prepared for each tested pH. Complementary contact angle measurements of water droplets onto pellets of

compressed particles, and glass slides (both pristine and modified with sodium alginate), immersed in 10 or 10,000 cSt silicone oils were also obtained. The surface tensions of both silicon oils were measured by pendant drop experiments using the same optical tensiometer.

2.4 Emulsions Preparation and Characterization

The emulsions were prepared in glass vials (i.d. 1.2 cm, h. 4.6 cm). The oil volume fraction ϕ_o was varied from 0.1 to 0.8, and the particle concentration from 2% to 12% ($g \cdot 100\ ml^{-1}$), at pH 7.0 for a total volume of 15 ml. Unless explicitly mentioned, the emulsions were all prepared by weighing the required mass of particles (0.6 g) in the glass vials, followed by the addition of the required volume of water. The oil phase was next added dropwise over 4 min and dispersed using an homogenizer operated at 24,000 rpm (Cole-Parmer LabGEN 125, equipped with a 0.5 cm (inner diameter) element). Once the oil was completely added, mixing was continued for another 2 min. The type of emulsion was determined by conductivity measurements (aqueous phase conductivity ≈ 0.7-3.5 μS; silicone oil phase conductivity = 0 μS) and by visual observation.

2.4.1 Optical Characterization of Emulsions

The emulsions droplets were visualized by dark field optical microscopy (Olympus BX51 by Cytoviva, Objectives = 10x and 50x Plan Fluorite, and 60x UPL Fluorite Oil, and 100x UPL Fluorite Oil Camera Q imaging, Retigna 2000R fast 1394, cooled color 12 bit). A drop of each emulsion was diluted with a drop of water at pH 7.0. The diluted emulsion was then spread on a microscope glass slide (Fisher Scientific). Photographs of the emulsions in glass vials were taken with a Nikon DX AF-S Nikkor 18-55mm 1:3.5-5.6 G camera.

2.4.2 Confocal Laser Scanning Microscopy (CLSM) Analysis

CLSM observations were realized with an Olympus IX 71 inverted confocal microscope (Olympus Canada Inc., Richmond Hill, ON, Canada) using 40x and 60x objective lenses (2048×2048 pixels resolution). 5-(4,6-dichlorotriazinyl)aminofluorescein (DTAF, D0531, Sigma-Aldrich) was covalently linked with SA. This dye was specifically chosen since it reacts directly with hydroxyl groups in aqueous solution at pH 9.0 and at room temperature to form covalent links with SA [47]. First, 10 mg of DTAF were added to 50 ml of Na_2CO_3-$NaHCO_3$ buffer solution (0.1 M, pH = 10.0). Next, 2.0 g of SA were dissolved in the DTAF solution, and the resulting solution was then left overnight to react at room temperature with stirring at 600-700 rpm. Finally, the reaction was stopped the following morning by adjusting the pH to 7.0. This value ensured quick diffusion of the counterions during the following dialysis step against Milli-Q water for 48 h to remove counterions and unreacted DTAF. Bacteria growth was inhibited with sodium azide (0.02 wt%) and the Milli-Q water was changed at 2 h intervals. Finally, a yellow powder was recovered after dialysis and freeze-drying (DTAF-labelled SA). The observation of fluorescent SP-SA particles was realized by recording the emission between 510 nm and 550 nm, by exciting DTAF at 488 nm.

3. Results

3.1 Zeta potential and contact angle measurements

Zeta potentials (ζ) and contact angles (θ) were measured as a function of pH for pristine (as received) silica particles (SP), silanized particles (SP-Sil, only for ζ) and particles modified with sodium alginate (SA) (SP-SA) (**Figure 1**).

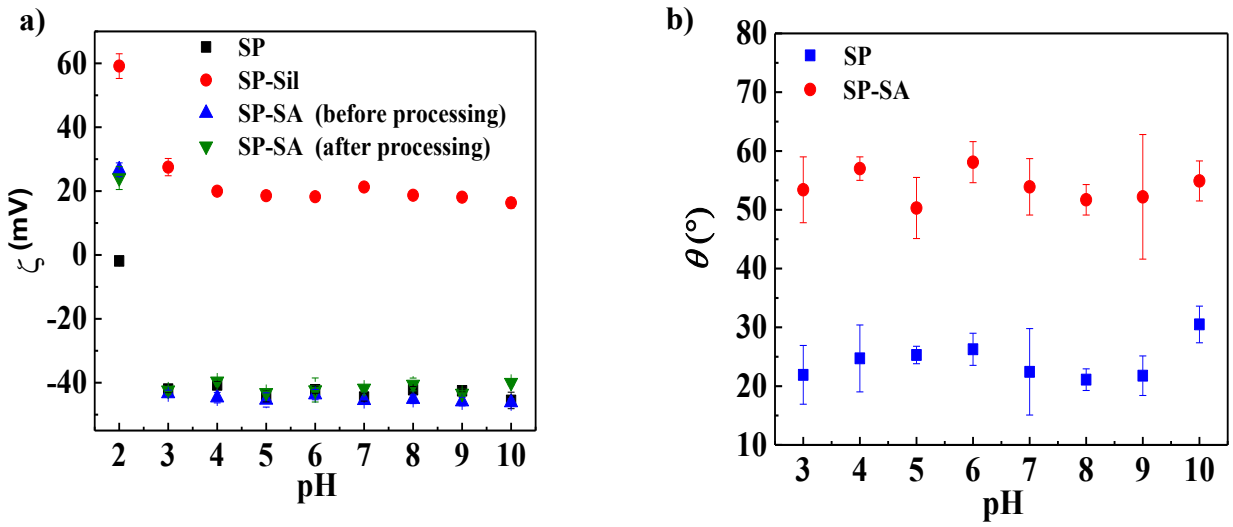

Figure 1. Values of zeta potentials ζ (a) and contact angles θ (b) as a function of pH (2.0 to 10.0), for the three types of silica particles: pristine (SP), silanized (SP-Sil), and grafted with sodium alginate (SP-SA).

SP particles possess a slightly negative ζ value at pH 2.0 that diminishes to a nearly constant negative values (-40 mV) as the pH increases from 3.0 to 10.0 (**Figure 1a**). This is explained by the deprotonation of hydroxyl groups (pKa= 3.5 [48]) on the particle surface as the pH increases [49]. SP-Sil particles display a positive ζ value of +58.0 mV at pH 2.0 due to the significant protonation of APTMS amino ($–NH_2$) groups at low pH. When the pH ranges from 3.0 to 10.0, an inferior and nearly constant positive ζ value of +25.0 mV is obtained. This is due to the deprotonation of the hydroxyl groups, and the gradual deprotonation of positively charged APTMS ($–NH_3^+$) groups to neutral $–NH_2$ groups, on the particle surface. Finally, at pH 2.0, SP-SA particles behave differently compared to SP particles, since ζ increased to +22.5 mV due to the protonation of both (–COOH) groups and remaining surface amino ($–NH_2$) groups. As the

pH increases, the gradual deprotonation of both amino groups and SA carboxylate groups (pKa = 3.5) results in a nearly constant ζ value of -40 mV, similar to SP. Furthermore, the homogenization processing of SP-SA particles did not alter the surface chemistry, since the ζ patterns of particles before and after processing are similar. These results confirm the grafting of the two silane reagents, followed by SA, with the surface-grafted APTMS. Similar results were obtained in a previous publication [40].

The wettability of SP and SP-SA particles was characterized via the contact angle (θ) of water droplets deposited onto the surface of compressed disks of particles, in air, over a pH range of 3.0 to 10.0 (**Figure 1b)**. On unmodified SP particles, θ increases from 22° to 30.5°, while the pH increases from 3.0 to 10.0. For SP-SA particles, θ increases above 50° and the particles become more hydrophobic compared to pristine particles (but more hydrophilic compared to SP-Sil particles, see [40]), which is due to a balance effect between the hydrophobic silanes and hydrophilic SA. The ζ and θ measurements confirm the surface modification of silica particles with both APTMS and TMPS silanes, followed by the coupling between SA and APTMS [42]. In complement, we have measured the contact angles of water droplets deposited onto pellets of compressed particles, and glass slides (to eliminate the effect of pellet surface roughness), for both pristine and sodium alginate modified surfaces, when immersed in 10 cSt or 10,000 cSt silicone oils (**Figure S1**, **Tables S1 and S2**). First, water droplets deposited onto pellets of compressed particles immersed in 10 cSt silicone oil display relatively similar trends to results in air (**Figure S1**): 74° ± 7° for pristine particles, 165° ± 13° for silanized particles, and 63° ± 4° for SA-modified particles, illustrating that we recover a more balanced

hydrophilic/hydrophobic behavior once the silanized particles are grafted with sodium alginate. Second, the water contact angles measured in both oils display systematically higher values compared to contact angles measured in air, indicating an affinity of the silicone oils for both the silica particles and glass slides due to their similar compositions.

Interestingly, the contact angles measured in the 10,000 cSt oil are also systematically superior (or nearly equal) to results in the 10 cSt oil. In complement, the surface tensions of both oils are quite comparable ($\gamma_{10\ cSt}$ = 20.8 ± 0.2 mN/m and $\gamma_{10,000\ cSt}$ = 22 ± 1 mN/m, **Table S3**). These results indicate a difference in particle wettability between the two oils, and suggest that the differences in emulsion stability observed between the 10 cSt and 10,000 cSt are of thermodynamic origin. However, at this point, the molecular origin of these differences remains unclear and will be addressed in a future publication. Interestingly, Avazpour et al. [50] recently demonstrated that a 10° difference in particle wettability can be enough to have a selective effect on particle adsorption.

3.2 Emulsion stabilization with pristine and modified silica particles

We first assessed the capacity of SP, SP-Sil and SP-SA particles to stabilize emulsions comprised of low and high viscosity silicone oils (SO, 10 and 10,000 cSt) and water (W) (**Figure 2**). Both SP and SP-SA particles stabilize oil-in-water emulsions with 10 cSt oil (**Figure 2a-b**). However, only SP-SA particles stabilize 10,000 cSt oil droplets (average droplet diameter d = 63 ± 26 μm), while the oil phase remains mostly un-emulsified and phase separated when using SP particles (**Figure 2c-d**) – this is one of the highest tested oil viscosity reported in the literature for the preparation of

Pickering emulsions. SP-Sil particles do not stabilize emulsions, most probably due to their significant hydrophobic character, as the contact angles show in the previous section.

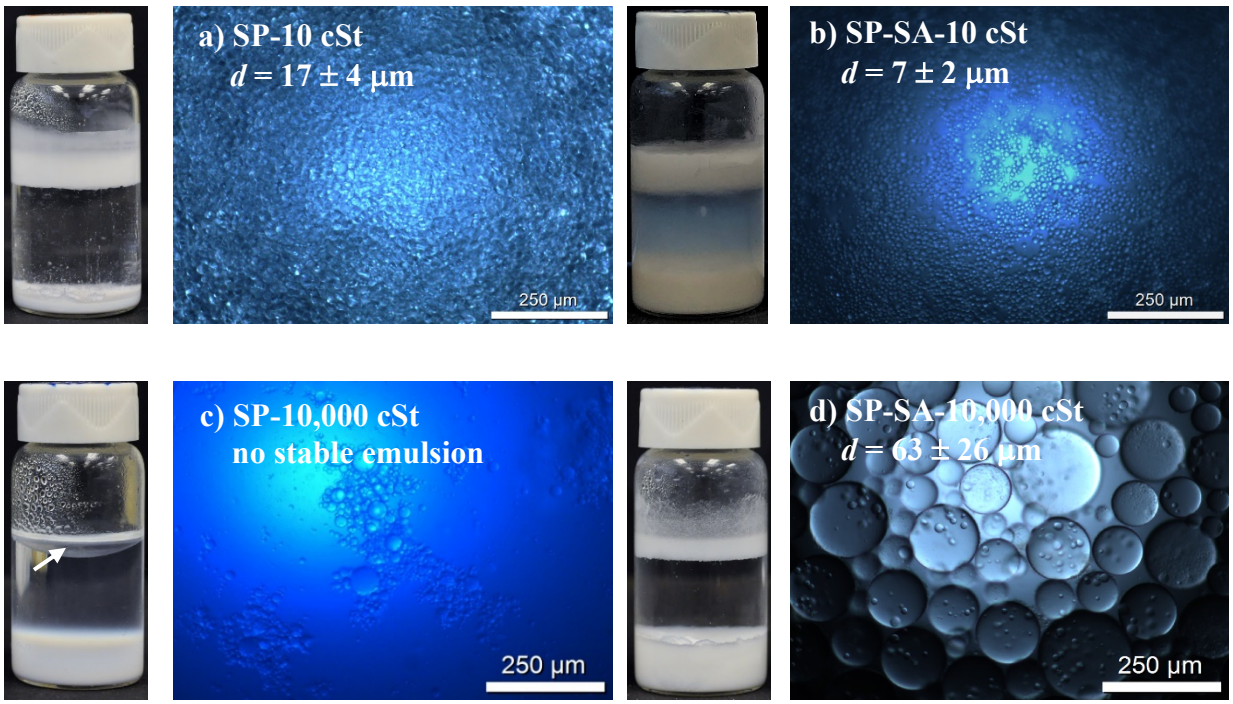

Figure 2. Macroscopic aspect and optical microscopy pictures of Pickering emulsions prepared with 4% particles (w/v) at $\phi_o = 0.1$: a) SP particles with 10 cSt oil; b) SP-SA particles with 10 cSt oil; c) SP particles with 10,000 cSt oil (un-emulsified oil indicated with white arrow); d) SP-SA particles with 10,000 cSt oil. Note that the sedimenting phase in a) and c) are very small emulsified silicon oil droplets (see **Figure S2**).

Looking at the microstructure, oil droplets obtained with the SP-SA particles and the 10,000 cSt oil show a significant amount of sub-inclusions within the droplets (see also **Supporting**

Information video file "Emulsion - 10_000 cSt oil.avi" showing flowing droplets with sub-inclusions). Such a feature is not observed in the 10 cSt oil droplets. This was an unexpected result, since multiple emulsions prepared with only one type of particles (here, SP-SA particles) have not been reported so far at such a high oil viscosity [23-24, 26, 28]. In the next section, oils of increasing viscosities are used to detect the onset of formation of these composite droplets using SP-SA particles.

3.3 Effect of oil viscosity on the formation of multiple emulsions

Figure 3 illustrates the effect of increasing oil viscosity from 1,000 to 30,000 cSt on droplet microstructure, for constant contents of SP-SA particles (4%) and oil volume fraction (ϕ_o = 0.1). Interestingly, stabilized oil droplets are observed even at such high oil viscosities. At 1,000 cSt and 5,000 cSt (**Figure 3a-b**), a few water droplets sub-inclusions can be observed (although not obvious, see white arrows in **Figure 3a and b**) in certain oil drops. The number and size of water droplets sub-inclusions significantly increases when the oil viscosity reaches 10,000 and 30,000 cSt (**Figure 3c-d**). At 10,000 cSt (**Figure 3c**), nearly all of the observed oil droplets contain sub-inclusions.

Viscosity is clearly a key-factor driving the formation of these multiple emulsions. In the next section, confocal laser scanning microscopy is employed to see if SP-SA particles are present at the surface of both oil droplets and water sub-inclusions.

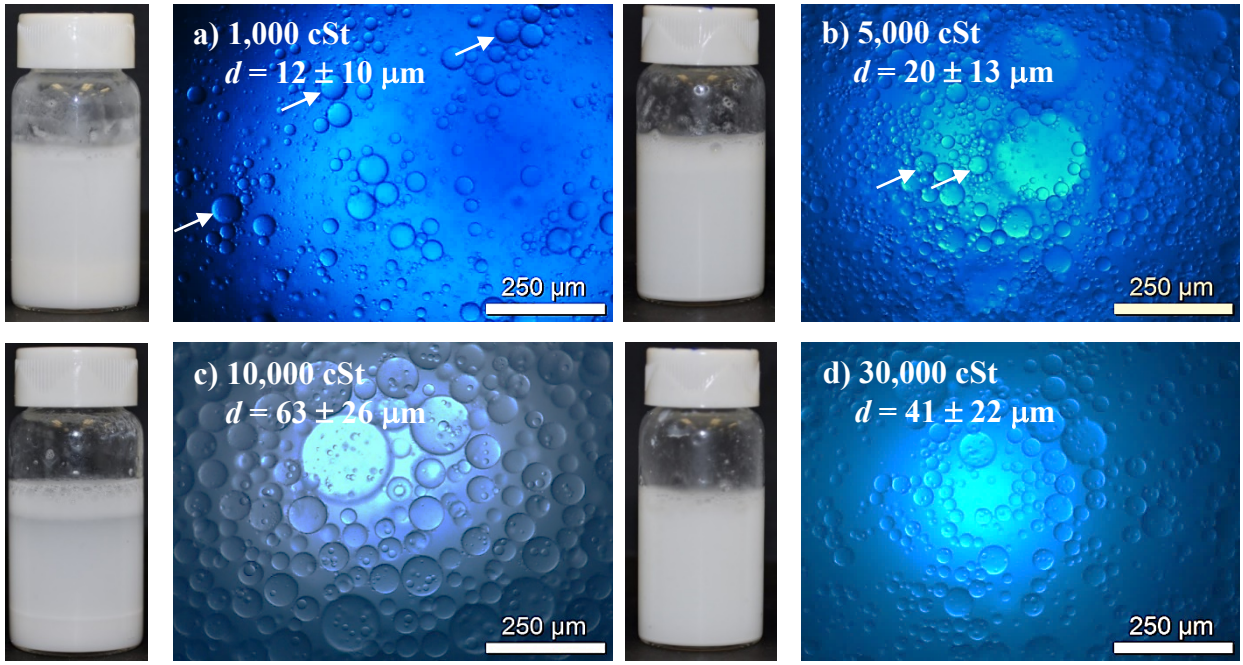

Figure 3. Effect of oil viscosity on the formation of multiple emulsions. Macroscopic (vials, pictures taken right after processing) and optical microscopy pictures (taken right after processing) of Pickering emulsions prepared with 4% SP-SA particles and ϕ_o = 0.1 silicone oil content, at pH = 7.0: a) 1,000 cSt; b) 5,000 cSt; c) 10,000 cSt and d) 30,000 cSt.

3.4 Internal drop microstructure investigated by confocal microscopy

In order to visualize the SP-SA particles by CLSM, the particles were tagged with DTAF**. Figure 4** clearly indicates that the particles are surface-active and form dense layers, both on the surface of the oil droplets, and at the surface of sub-inclusions – indicating that the sub-inclusions are comprised of water. This means that these SP-SA particles can indeed stabilize both O/W and W/O emulsions, even though previous work [40] shows that they prefer the former conformation.

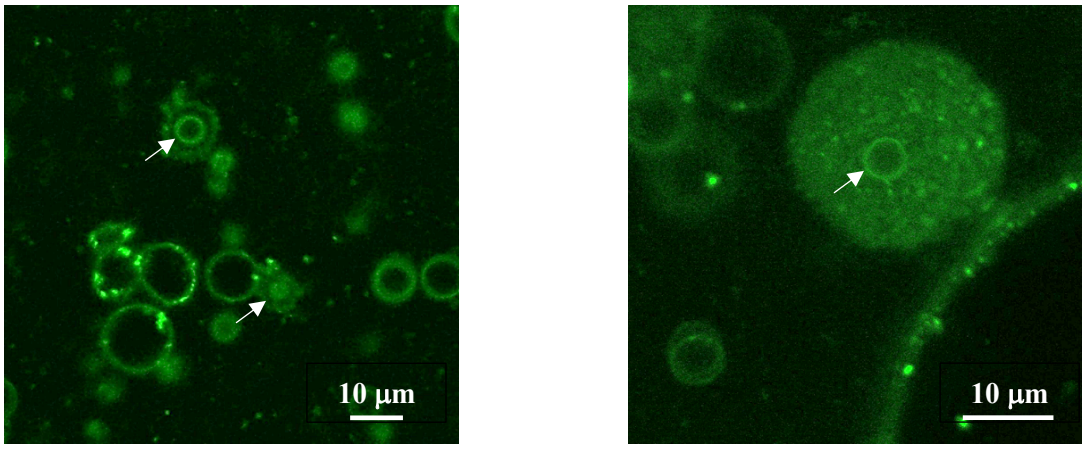

Figure 4. CLSM pictures of Pickering emulsions (ϕ_o = 0.1, 10,000 cSt) with 4% (wt/vol) SP-SA particles tagged with DTAF, showing the interfacial adsorption of particles both at the oil surface and water sub-inclusions (indicated with white arrows in the latter case). Note that the particles contained inside the drop on the right are most probably a 2D projection of the particles covering the top of a droplet (spherical cap).

3.5 Effects of oil and particle concentrations

To investigate the effect of oil and water contents on the formation of these double emulsions, four different oil volume fractions were compared (for the 10,000 cSt silicone oil), namely ϕ_o = 0.05, 0.1, 0.2 and 0.3, at a constant particle content of 4% (w/v). The results are shown in **Figure 5**. At ϕ_o = 0.05 (**Figure 5a**), most of the oil phase was emulsified, and multiple droplets were obtained. Increasing the silicone oil fraction to ϕ_o = 0.1 also resulted in the formation of multiple droplets, and further increasing ϕ_o to 0.2 and 0.3 led to an apparent wider size distribution. All emulsions exhibited sub-inclusions. In other words, the amount of oil seems to have no significant effect on the amount or size of sub-inclusions.

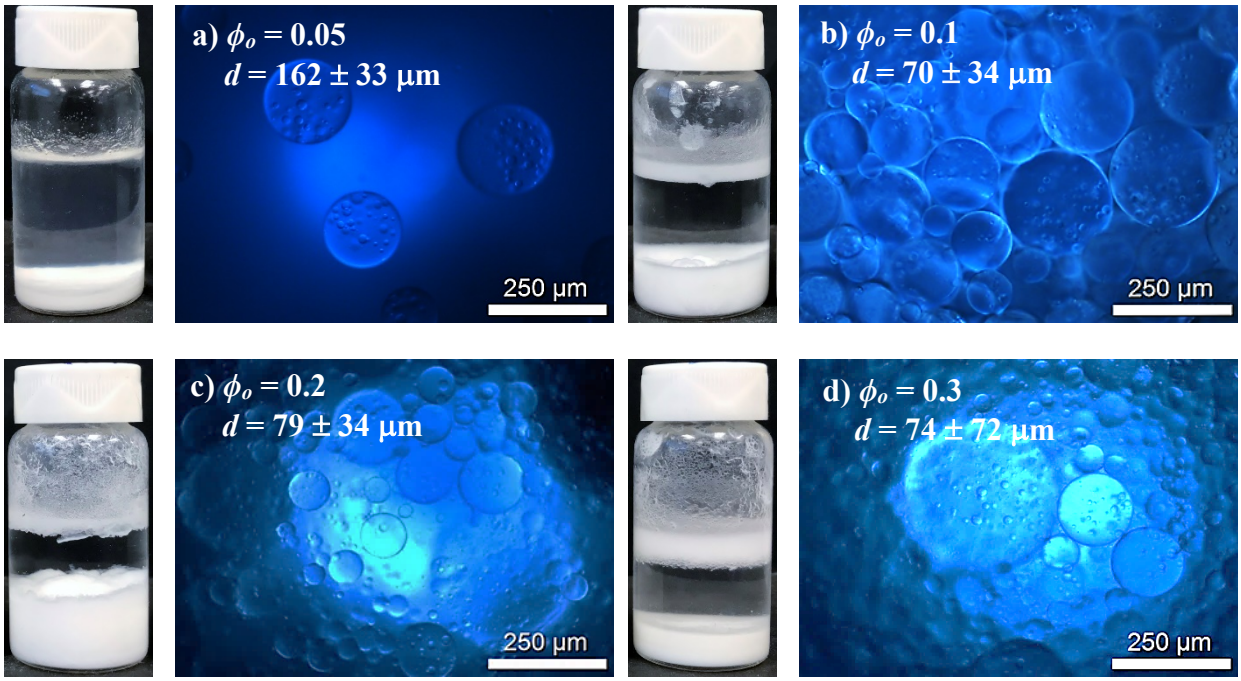

Figure 5. Effect of oil fraction ϕ_o on the formation of multiple emulsions comprised of 4% (w/v) SP-SA particles and 10,000 cSt silicone oil, at pH = 7.0 (micrographs taken right after processing): a) ϕ_o = 0.05; b) ϕ_o = 0.1; c) ϕ_o = 0.2 and d) ϕ_o = 0.3 (d). Vials display emulsion stability after 10 months.

A similar conclusion is reached when the particle content is varied, at a constant oil content. **Figure 6** illustrates the internal structure of oil droplets (10,000 cSt silicone oil, ϕ_o = 0.1) when the particle concentration increases from 2% to 12% (w/v). Again, we can see that increasing the particle content does not have a significant impact on the number and size of water sub-inclusions in the oil droplets (except at 12% content, where we can see more smaller droplets without sub-inclusions), even though it has an impact on the macroscopic appearance of the emulsions. We then next investigated the effects of three processing parameters: (1) the duration of oil addition, (2) the processing time and (3) the components mixing sequence.

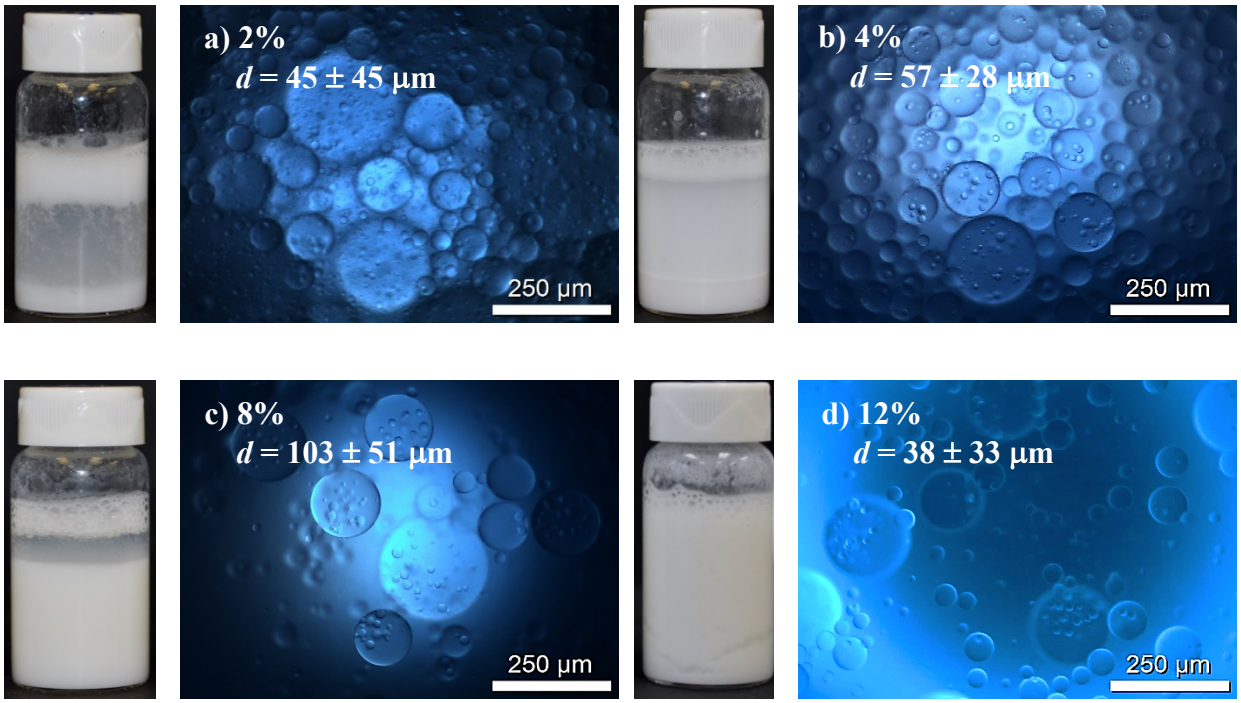

Figure 6. Effect of particle concentration on the oil droplets internal structure in emulsions prepared with SP-SA particles (w/v) with 10,000 cSt silicone oil (ϕ_o = 0.1) at pH = 7.0 : a) 2% particles (w/v); b) 4%; c) 6% and d) 12%. Micrographs and vial pictures taken right after processing.

3.6 Effects of processing variables: duration of oil addition, processing time, and sequence of mixing

The effect of silicone oil addition duration is illustrated in **Figure S3**, for emulsions comprised of 4% particles and 10,000 cSt oil (ϕ_o = 0.1). Adding the oil in 1 min (+ 5 minutes of additional processing time) or 6 min (with no additional processing time) does not significantly alter the internal oil droplet structure in terms of water sub-inclusion number and size. If the duration of oil addition instead is kept constant at 4 min, while the additional processing time is varied – 2 min vs 8 min –, again no clear difference is observed, as **Figure S4** shows.

This led us to look at the sequence of components addition (**Figure 7**). Until now, the particles were first added to water, and the oil phase was gradually added to form an O/W emulsion. In **Figure 7a-b**, the particles were first mixed with water, and the resulting suspension was gradually added to the minor oil phase while homogenizing (final composition: $\phi_o = 0.2$). In the second row, **Figure 7c-d**, the particles were dispersed first in the oil phase, and water was gradually added subsequently (final composition: $\phi_o = 0.2$). In **Figure 7a and c,** mixing was stopped right after phase inversion (right after the formation of an O/W emulsion), when water becomes the continuous phase, while in **Figure 7b and d**, mixing is continued for 2 min after the complete addition of the aqueous particle suspension (b) or water (d). In all cases, we observe that the oil droplets contain a large number of very small water droplets sub-inclusions (**Figure 7b and c** are particularly striking), contrasting sharply with the previous results, which showed less but larger sub-inclusions. This indicates that phase inversion probably plays an important role during the formation of these multiple emulsions, while further processing after phase inversion does not affect significantly the sub-inclusions (at least for a short additional processing time).

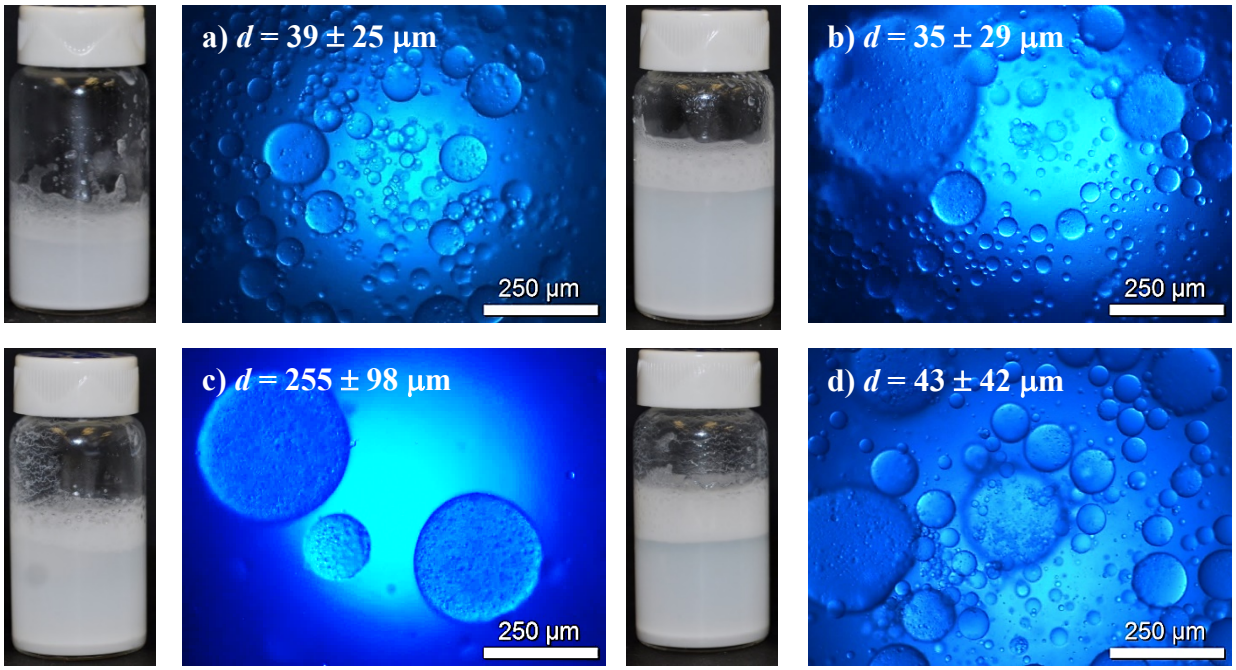

Figure 7. Effect of mixing sequence on Pickering emulsions appearance and microstructure, prepared with 4% (w/v) SP-SA particles and 10,000 cSt oil at pH = 7.0. In (a, b), particles are first dispersed in water, then the aqueous suspension is gradually added in oil while homogenizing: a) processing stopped when phase inversion occurs (oil-in-water emulsion is formed); b) homogenizing is prolonged 2 min after the complete addition of particle suspension (ϕ_o = 0.2). In (c, d), particles are first dispersed in the oil phase, then water is gradually added in the (oil + particle) suspension while homogenizing: c) process stopped after phase inversion occurs; d) homogenizing is prolonged 2 min after complete addition of water (ϕ_o = 0.2).

4. Proposed mechanism for the formation of multiple Pickering emulsions

By modifying the surface chemistry of silica particles with a natural polysaccharide, in this case sodium alginate, and by using highly viscous silicone oils, we have promoted the formation of multiple (W/O/W) Pickering emulsions via a one step process – this contrasts sharply with the more traditional approach using two types of particles/surfactants, and two successive mixing steps. Viscosity clearly plays an important role, since multiple emulsions are only significantly formed for 10,000 and 30,000 cSt oils (**Figure 3**). CLSM observations also reveal that SP-SA

particles cover both interfaces – the outer oil-water interface of the primary emulsion, and the water-oil interface associated to water sub-inclusions (**Figure 4**). This can be explained by the SP-SA particulates "intermediate" wettability – less hydrophilic than the pristine SP particles, but more hydrophilic compared to the silane grafted particles (SP-Sil) (**Figure 1**).

It is pertinent to note that the oil volume fraction and particle content do not have a significant impact on the sub-inclusions size and number when the oil is added dropwise to the major water phase containing particles (**Figures 5 and 6**) – suggesting coalescence does not play a significant role. However, when water (with or without particles) is added dropwise to the minor oil phase until phase inversion occurs, the internal structure of the oil droplets reveals a high number of smaller water droplets sub-inclusions, that remain trapped in the oil phase as processing continues (at least for a few minutes, **Figure 7**). Clearly, phase inversion can play an important role. When emulsions are prepared by adding dropwise the aqueous phase (**Figure 7**), water droplets are dispersed in the oil phase and are stabilized by SP-SA particles, forming the first emulsion. When catastrophic phase inversion occurs (when the water volume fraction goes over 55 vol%), the oil-in-water emulsion is formed, and the initial water droplets in the oil phase remain trapped in the oil droplets (see **Figure S5**). We believe that this phenomenon is due to (1) the reduced mobility of droplets in a very viscous liquid, and (2) to the shell of particles formed at the surface of the oil droplets – explaining the persistence of sub-inclusions when processing is prolonged.

In the case when the oil phase is added dropwise (with oil being the minor (and ultimately) dispersed phase, **Figures 3**, **5** and **6**), water sub-inclusions are rapidly formed in the highly viscous and initially large oil droplets by an "engulfing" mechanism, before the oil droplets significantly reduce in size (due to the high viscosity, oil droplets are larger and more difficult to form), which would explain why fewer sub-inclusions are observed for these processing conditions. To verify

this hypothesis, we have taken emulsion samples right after the addition of the first, and second, drops of oil (10-20 seconds and 30-40 seconds, respectively, after processing begins) (**Figure S6**). Optical microscopy micrographs show that no sub-inclusions are observed early in the process (right after the addition of the first drop of oil, Figure S6a), while sub-inclusions are seen after the second drop of oil has been added (Figure S6b). Schematic illustrations explaining the formation of multiple emulsions via gradual water addition and phase inversion, or by gradual oil addition, are presented in **Figure 8**.

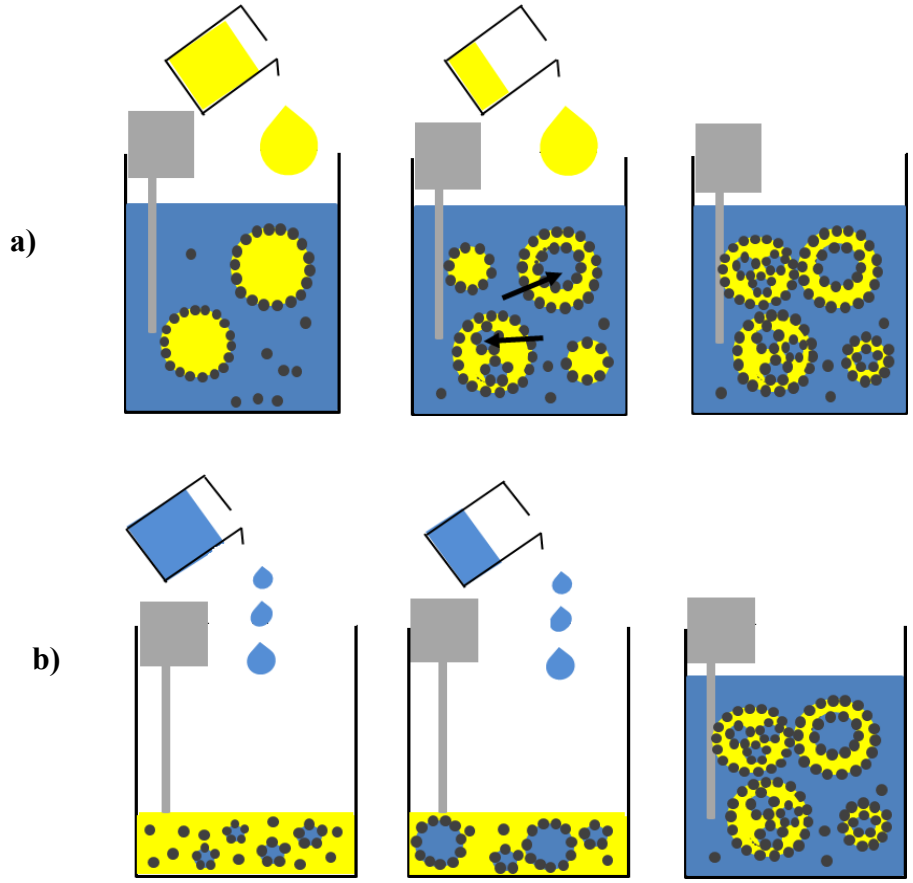

Figure 8. a) Schematic illustrations of the formation of multiple emulsions by gradual oil addition. First, large droplets of oil are formed due to intense mixing (homogenizer in grey) and small water droplets are transferred or "engulfed" into the oil droplets; b) In comparison, gradual water addition results in the dispersion of water droplets. As water addition increases, phase inversion happens and oil droplets are now dispersed, retaining water sub-inclusions.

The formation of sub-inclusions via phase inversion in highly viscous systems has been reported in binary melt-processed polymer blends of polypropylene/polycarbonate and polyethylene copolymer/polyamide by Favis et al. [51-53]. They found that increasing the viscosity of the dispersed phase (polypropylene) caused an increase in the concentration of sub-inclusion droplets because of the lower sub-inclusion droplets mobility – also resulting in a higher retention of sub-inclusions in the dispersed phase. Interestingly, they were also able to increase significantly the number of sub-inclusions in polyamide droplets via a phase inversion process during the processing of polyethylene copolymer/polyamide blends, like we demonstrate in **Figure 7**. By prolonging the mixing time, they demonstrated that the sub-inclusions gradually migrated to the matrix phase – unlike our system, the polymer droplets were not covered with particulates shells preventing the transfer of sub-inclusions. Regarding the formation of sub-inclusions in emulsions, previous works underlined that when steady-state is achieved, the number of sub-inclusions entering the dispersed phase droplets (via droplet-droplet coalescence) should be balanced by the sub-inclusions escaping the droplets [54-56]. Droplet escape should then be more difficult as the viscosity of the dispersed phase increases – this is indeed what we observe in our systems, since sub-inclusions are only observed with high viscosity oils. However, the formation of sub-inclusions occurs early during processing even at very low volume fractions of dispersed phase, which appears more difficult to explain solely via a droplet-droplet coalescence mechanism. Finally, this approach represents an interesting and simple strategy to prepare multiple emulsions with a minimum number of components.

5. Conclusion

Viscosity plays an important role when designing and scaling up processes in chemical engineering. While a few articles have looked at the effect of the dispersed phase viscosity on the

formation of Pickering emulsions (over a range of 10 to 5,000 cSt), the few reports available typically conclude that the amount of emulsified dispersed phase decreases as viscosity increases [34-37], when all other parameters are kept constant – which is intuitively expected.

In this work, we demonstrate that viscosity can also play a significant microstructuring role when processing Pickering emulsions. We have prepared, in a one-step process by simultaneously mixing all components, multiple (W/O/W) Pickering emulsions using highly viscous silicone oils and a single type of sub-μm silica particles surface-modified with two silanes, and sodium alginate. The technique we present necessitates a minimum number of steps and components – in particular, no additional types of particulates or surfactants are employed, nor particulates with complex structures and/or surface chemistries. Oil viscosity controls the formation of water sub-inclusions, which are only observed when the oil viscosity is equal or superior to 10,000 cSt. Furthermore, the formation of sub-inclusions is enhanced when phase inversion occurs during processing, when water is added dropwise to the oil [27]. Finally, both the water sub-inclusions/oil droplets, and oil droplets/continuous aqueous phase interfaces, are covered with particles, indicating a balance of hydrophilic/hydrophobic properties.

The high viscosity of the oil phase, combined with the particulate barriers at the interfaces, contribute in stabilizing the water sub-inclusions, and in inhibiting their transfer in the continuous aqueous phase during processing. The mechanism is highly reminiscent of sub-inclusions formation in highly viscous melt-processed polymer blends, in which phase inversion during processing can lead to the kinetic trapping of sub-inclusions in the dispersed phase [51-53]. However, since no particles are present at interfaces in this case, the sub-inclusions gradually migrate to the continuous phase with mixing time. Further investigations are required at this point

to understand what controls the viscosity threshold over which sub-inclusions start to appear, and how their amount and size can be controlled.

Acknowledgements

We acknowledge the financial support of Imperial Oil through a University Research Award grant, Total (Industrial Research Chair), the National Sciences and Engineering Research Council (Discovery Grant), CREPEC (Projets Structurants), Polytechnique Montreal (UPIR undergraduate research grants) and the Canada Foundation for Innovation (John R. Evans Leaders Fund). We would like to thank Dr. Chang-Sheng Wang for confocal microscopy observations.

References

[1] N. Garti, Double emulsions - Scope, limitations and new achievements, Colloid Surface A 123 (1997) 233-246.

[2] B.P. Binks, S.O. Lumsdon, Stability of oil-in-water emulsions stabilised by silica particles, PCCP 1(12) (1999) 3007-3016.

[3] K. Lindenstruth, B.W. Muller, W/O/W multiple emulsions with diclofenac sodium, Eur J Pharm Biopharm 58(3) (2004) 621-7.

[4] M. Gallarate, M.E. Carlotti, M. Trotta, S. Bovo, On the stability of ascorbic acid in emulsified systems for topical and cosmetic use, Int. J. Pharm. 188(2) (1999) 233-241.

[5] K. Miyazawa, I. Yajima, I. Kaneda, T. Yanaki, Preparation of a new soft capsule for cosmetics, J Cosmet Sci 51(4) (2000) 239-252.

[6] A. Aserin, Multiple Emulsion: Technology and Applications, 1st ed., Wiley-Interscience2007.

[7] L. Liu, W. Wang, X.J. Ju, R. Xie, L.Y. Chu, Smart thermo-triggered squirting capsules for nanoparticle delivery, Soft Matter 6(16) (2010) 3759-3763.

[8] A. Vaziri, B. Warburton, Slow-Release of Chloroquine Phosphate from Multiple Taste-Masked W/O/W Multiple Emulsions, J. Microencapsulation 11(6) (1994) 641-648.

[9] S. Zheng, Y. Zheng, R.L. Beissinger, D.T. Wasan, D.L. McCormick, Hemoglobin multiple emulsion as an oxygen delivery system, Biochimica et Biophysica Acta (BBA) - General Subjects 1158(1) (1993) 65-74.

[10] L. Hong, G. Sun, J. Cai, T. Ngai, One-step formation of w/o/w multiple emulsions stabilized by single amphiphilic block copolymers, Langmuir 28(5) (2012) 2332-6.

[11] C.A. Dorval Dion, W. Raphael, E. Tong, J.R. Tavares, Photo-initiated chemical vapor deposition of thin films using syngas for the functionalization of surfaces at room temperature and near-atmospheric pressure, Surface & Coatings Technology 244 (2014) 98-108.

[12] D.S. Wen, Y.L. Ding, Effective thermal conductivity of aqueous suspensions of carbon nanotubes (carbon nanotubes nanofluids), J. Thermophys Heat Transfer 18(4) (2004) 481-485.

[13] Y. Zhu, J. Sun, C. Yi, W. Wei, X. Liu, One-step formation of multiple Pickering emulsions stabilized by self-assembled poly(dodecyl acrylate-co-acrylic acid) nanoparticles, Soft Matter 12(36) (2016) 7577-7584.

[14] S. Sacanna, W.K. Kegel, A.P. Philipse, Thermodynamically stable pickering emulsions, Phys. Rev. Lett. 98(15) (2007) 158301.

[15] K.L. Thompson, C.J. Mable, J.A. Lane, M.J. Derry, Fielding, L. A., S.P. Armes, Preparation of Pickering Double Emulsions Using Block Copolymer Worms, Langmuir 31(14) (2015) 4137-4144.

[16] J. Frelichowska, M.A. Bolzinger, Y. Chevalier, Pickering emulsions with bare silica, Colloids and Surfaces A: Physicochemical and Engineering Aspects 343(1-3) (2009) 70-74.

[17] S.M. Y. Sela, N. Garti, Polymeric surfactants based on polysiloxanes—graft-poly (oxyethylene) for stabilization of multiple emulsions, Colloid Surface A 83(2) 143-150.

[18] A.S. Utada, E. Lorenceau, D.R. Link, P.D. Kaplan, H.A. Stone, D.A. Weitz, Monodisperse double emulsions generated from a microcapillary device, Science 308(5721) (2005) 537-41.

[19] H.C. Shum, Y.J. Zhao, S.H. Kim, D.A. Weitz, Multicompartment polymersomes from double emulsions, Angew. Chem. Int. Ed. Engl. 50(7) (2011) 1648-51.

[20] D. Lee, D.A. Weitz, Double emulsion-templated nanoparticle colloidosomes with selective permeability, Adv. Mater. 20(18) (2008) 3498.

[21] Z.H. Nie, S.Q. Xu, M. Seo, P.C. Lewis, E. Kumacheva, Polymer particles with various shapes and morphologies produced in continuous microfluidic reactors, J. Am. Chem. Soc. 127(22) (2005) 8058-8063.

[22] S. Kim, K. Kim, S.Q. Choi, Controllable one-step double emulsion formation via phase inversion, Soft Matter 14(7) (2018) 1094-1099.
[23] F. Tu, D. Lee, One-step encapsulation and triggered release based on Janus particle-stabilized multiple emulsions, Chem Commun (Camb) 50(98) (2014) 15549-52.
[24] B.P. Binks, C.P. Whitby, Silica particle-stabilized emulsions of silicone oil and water: aspects of emulsification, Langmuir 20(4) (2004) 1130-7.
[25] K.A. White, A.B. Schofield, P. Wormald, J.W. Tavacoli, B.P. Binks, P.S. Clegg, Inversion of particle-stabilized emulsions of partially miscible liquids by mild drying of modified silica particles, J. Colloid Interface Sci. 359(1) (2011) 126-35.
[26] Y. Nonomura, N. Kobayashi, N. Nakagawa, Multiple pickering emulsions stabilized by microbowls, Langmuir 27(8) (2011) 4557-62.
[27] B.P. Binks, P.D. Fletcher, B.L. Holt, P. Beaussoubre, K. Wong, Phase inversion of particle-stabilised perfume oil-water emulsions: experiment and theory, Phys. Chem. Chem. Phys. 12(38) (2010) 11954-66.
[28] B.P. Binks, J.A. Rodrigues, Types of phase inversion of silica particle stabilized emulsions containing triglyceride oil, Langmuir 19(12) (2003) 4905-4912.
[29] A.G. Cunha, J.B. Mougel, B. Cathala, L.A. Berglund, I. Capron, Preparation of double Pickering emulsions stabilized by chemically tailored nanocelluloses, Langmuir 30(31) (2014) 9327-35.
[30] S. Frasch-Melnik, F. Spyropoulos, I.T. Norton, W1/O/W2 double emulsions stabilised by fat crystals--formulation, stability and salt release, J. Colloid Interface Sci. 350(1) (2010) 178-85.
[31] M. Williams, N.J. Warren, L.A. Fielding, S.P. Armes, P. Verstraete, J. Smets, Preparation of double emulsions using hybrid polymer/silica particles: new pickering emulsifiers with adjustable surface wettability, ACS Appl Mater Interfaces 6(23) (2014) 20919-27.
[32] B.P. Binks, R. Murakami, S.P. Armes, S. Fujii, Temperature-induced inversion of nanoparticle-stabilized emulsions, Angew. Chem. Int. Ed. Engl. 44(30) (2005) 4795-8.
[33] J.M. Morais, P.A. Rocha-Filho, D.J. Burgess, Influence of phase inversion on the formation and stability of one-step multiple emulsions, Langmuir 25(14) (2009) 7954-61.
[34] C.O. Fournier, L. Fradette, P.A. Tanguy, Effect of dispersed phase viscosity on solid-stabilized emulsions, Chemical Engineering Research & Design 87(4a) (2009) 499-506.

[35] E. Tsabet, L. Fradette, Study of the properties of oil, particles, and water on particle adsorption dynamics at an oil/water interface using the colloidal probe technique, Chemical Engineering Research & Design 109 (2016) 307-316.

[36] E. Tsabet, L. Fradette, Effect of the properties of oil, particles, and water on the production of Pickering emulsions, Chem. Eng. Res. Des. 97 (2015) 9-17.

[37] E. Tsabet, L. Fradette, Semiempirical Approach for Predicting the Mean Size of SolidStabilized Emulsions, Ind. Eng. Chem. Res 54 (2015) 11661−11677.

[38] Y.H. Liu, E.L. Carter, G.V. Gordon, Q.J. Feng, S.E. Friberg, An investigation into the relationship between catastrophic inversion and emulsion phase behaviors, Colloid Surface A 399 (2012) 25-34.

[39] E. Tsabet, L. Fradette, Effect of Processing Parameters on the Production of Pickering Emulsions, Industrial & Engineering Chemistry Research 54(7) (2015) 2227-2236.

[40] F. Sabri, K. Berthomier, C.-S. Wang, L. Fradette, J.R. Tavares, N. Virgilio, Tuning particle–particle interactions to control Pickering emulsions constituents separation, Green Chemistry 21(5) (2019) 1065-1074.

[41] T. Harnsilawat, R. Pongsawatmanit, D.J. McClements, Characterization of beta-lactoglobulin-sodium alginate interactions in aqueous solutions: A calorimetry, light scattering, electrophoretic mobility and solubility study, Food Hydrocolloids 20(5) (2006) 577-585.

[42] F. Sabri, K. Berthomier, A. Marion, L. Fradette, J.R. Tavares, N. Virgilio, Sodium alginate-grafted submicrometer particles display enhanced reversible aggregation/disaggregation properties, Carbohydr. Polym. 194 (2018) 61-68.

[43] B. Arkles, Silane Coupling Agents: Connecting Across Boundaries, in: I. Gelest (Ed.) 2006.

[44] K.L. Pickering, S. Raa Khimi, S. Ilanko, The effect of silane coupling agent on iron sand for use in magnetorheological elastomers Part 1: Surface chemical modification and characterization, Composites Part A: Applied Science and Manufacturing 68 (2015) 377-386.

[45] G. Giani, S. Fedi, R. Barbucci, Hybrid Magnetic Hydrogel: A Potential System for Controlled Drug Delivery by Means of Alternating Magnetic Fields, Polymers 4(4) (2012) 1157-1169.

[46] M. Lattuada, T.A. Hatton, Functionalization of monodisperse magnetic nanoparticles, Langmuir 23(4) (2007) 2158-2168.

[47] G. M.S., Advanced fluorescence reporters in chemistry and biology I, Springer, Berlin Heidelberg, 2010.

[48] K. Leung, I.M.B. Nielsen, L.J. Criscenti, Elucidating the Bimodal Acid-Base Behavior of the Water-Silica Interface from First Principles, J. Am. Chem. Soc. 131(51) (2009) 18358-18365.
[49] B. Knoblich, T. Gerber, Aggregation in SiO_2 sols from sodium silicate solutions, J. Non-Cryst. Solids 283(1-3) (2001) 109-113.
[50] R. Avazpour, M. Latifi, J. Chaouki, L. Fradette, Physical beneficiation of rare earth-bearing ores by Pickering emulsification, Minerals Engineering 144 (2019) 106034.
[51] B.D. Favis, C. Lavallee, A. Derdouri, Preparation of Composite Dispersed Phase Morphologies in Incompatible and Compatible Blends during Melt Processing, Journal of Materials Science 27(15) (1992) 4211-4218.
[52] B.D. Favis, and J. P. Chalifoux, Influence of composition on the morphology of polypropylyne/polycarbonate blends, Polymer 29 (1988) 1761-1767.
[53] B.D. Favis, and D. Therrien, Factors influencing structure formation and phase size in an immiscible polymer blend of polycarbonate and polypropylene prepared by twin-screw extrusion, Polymer 32(8) (1990) 1474-1481.
[54] F. Groeneweg, W. G. M. Agterof, P. Jaeger, J. J. M. Janssen, J. A. Wieringa, J. K. Klahn, On the Mechanism of the Inversion of Emulsions, Chem. Eng. Res. Des. 76 (1998) 55-63.
[55] J. K. Klahn, J. J. M. Janssen, G. E. J. Vaessen, R. de Swart, W. G. M. Agterof, On the escape process during phase inversion of an emulsion, Colloids and Surfaces A: Physicochem. Eng. Aspects 210 (2002) 167-181.
[56] L. Liu, O. K. Matar, C. J. Lawrence, G. F. Hewitt, Laser-induced fluorescence (LIF) studies of liquid-liquid flows. Part I: Flow structures and phase inversion, Chem. Eng. Sci. 61 (2006) 4007-4021.